Quantum Electronics **37** (10) 910 – 915 (2007)

PACS numbers: 42.55.Rz; 42.55.Xi; 42.60.Lh
DOI: 10.1070/QE2007v037n10ABEH013666

Study of the possibility of developing a multichannel-diode-pumped multikilowatt solid-state laser based on optically dense active media

S.V. Garnov, V.A. Mikhailov, R.V. Serov, V.A. Smirnov, V.B. Tsvetkov, I.A. Shcherbakov

***Abstract*.** **Optimal conditions are determined for the development of efficient diode-pumped 1-μm solid-state lasers with output powers up to a few tens of kilowatts. The thermal operating conditions are analysed for various Yb^{3+}- or Nd^{3+}-doped active media used in high-power laser systems. The advantages and disadvantages of these active ions and various crystal matrices are discussed. The theoretical analysis and experimental simulations allow one to determine the application fields of various laser crystals. A new concept of a multibeam (multipoint) pumping of active media is proposed.**

Keywords: *high-average power lasers, diode pumping, optically dense active media, Nd : GdVO₄.*

1. Introduction

Lasers with output powers from one hundred watts up to a few tens of kilowatts are required for scientific studies and technological applications. Until recently the output power exceeding a few kilowatts during a prolonged operation was mainly obtained by using chemical or gas lasers emitting at $\lambda \sim 10$ μm, which have found wide industrial applications. However, emission at ~ 1 μm is preferable for many applications. As the output power of laser diodes is being increased, their reliability improved, and their cost reduced, diode-pumped high-power fibre and solid-state lasers began compete with existing technological lasers. The specific features of solid-state and fibre laser systems such as their compactness and simplicity are also their advantage. However, fibre lasers can be used, as a rule, in the cw regime. In addition, in the development of high-power fibre lasers, as by the way, of any lasers emitting high-beam-quality radiation, the problem of coherent combination of several sources appears.

At present the maximum output power emitted by a single fibre laser does not exceed, as a rule, ~ 2 kW. To achieve higher output powers by retaining the high quality of a laser beam, it is necessary to perform coherent combination of several individual fibre lasers. This problem has not been solved so far. Note that the coherent combination of laser beams is successfully performed for slab lasers. Thus, a laser setup based on slab lasers emitting a 25-kW high-quality beam (the divergence is less than 1.5 of the diffraction limit) is described in [1], and a 19-kW slab laser emitting a beam with the divergence equal to 1.73 of the diffraction limit is developed in [2]. However, such lasers have a complicated design and require a separate 'clean' room, so that the possibility of their practical applications seems restricted. The same concerns lasers operating on the 'heat capacity' of active elements, which can generate the 25-kW radiation only no longer than for 10 s or 67 kW only during 'short switching on' [1].

The aim of our study is to determine conditions for the development of highly efficient diode-pumped 1-μm solid-state lasers which can emit high-quality radiation both in the cw and pulsed regimes with the average output power up to a few tens of kilowatts. Unlike lasers described in the literature, we consider spatially separated diode pumping with a fibre pigtail and an optically dense crystal disc as an active medium. The high optical density, providing absorption of the pump radiation for two – three transits even in a thin active element, is achieved due to the high oscillator strength at the pump wavelength or due to a high concentration of lasing ions. This allows one to discard a complicated multipass pumping. The limiting possibilities of lasers built according to this scheme are analysed. Experiments are performed that confirm the conclusions of our analysis.

Note that the concept of optically dense active media has long been developed [3]. Thus, for flashlamp-pumped chromium- and neodymium-doped mixed garnet crystals, the record absolute (10.5 %) and slope (11.5 %) efficiencies were obtained upon free-running lasing and also the record slope efficiency (6 %) in the *Q*-switching regime. In addition, it has been shown experimentally that the pump damage threshold for an optically dense active medium considerably exceeds that for media with low optical densities (in the case of the uniform heat release [3]).

Note that, while in the case of flashlamp-pumped chromium-doped scandium garnet crystals we are dealing with the optically dense active medium with the high spectrally average absorption coefficient, in the case of diode pumping, we consider a 'pure' optically dense medium strongly absorbing at the pump wavelength. Such a medium (neodymium-doped gadolinium vanadate crystals) was proposed in [4]. Figure 1 presents the absorption spectra of $Nd : GdVO_4$ crystals for radiation with π- and σ-polar-

S.V. Garnov, V.A. Mikhailov, R.V. Serov, V.A. Smirnov, V.B. Tsvetkov, I.A. Shcherbakov A.M. Prokhorov General Physics Institute, Russian Academy of Sciences, ul. Vavilova 38, 119991 Moscow, Russia;
e-mail: tsvetkov@lsk.gpi.ru

Received 10 July 2007
Kvantovaya Elektronika **37** (10) 910 – 915 (2007)
Translated by M.N. Sapozhnikov

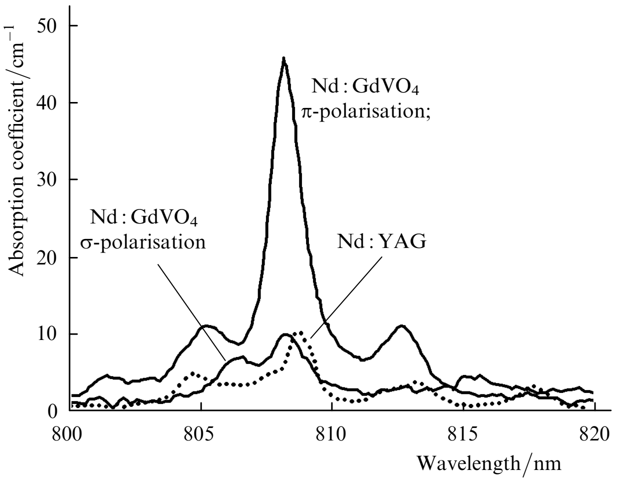

Figure 1. Absorption spectra of the Nd : GdVO$_4$ crystal (concentration of neodymium ions is 1 at%) for π- and σ-polarised radiations, and the absorption spectrum of the Nd : YAG crystal.

isations (the atomic concentration of Nd^{3+} ions was 1 %) and the absorption spectrum of a Nd : YAG crystal. One can see that the absorption coefficient for radiation with the π-polarisation at the pump wavelength achieves 45 cm^{-1}. At present high-quality Nd : GdVO$_4$ crystals with the absorption coefficient exceeding 100 cm^{-1} can be grown. With such an absorption coefficient, 99 % of the pump radiation is absorbed per one transit in the active-medium disc of thickness ~0.5 mm only.

Note that the development of high-power solid-state lasers is a challenging physical and technological problem. To solve this problem, it is necessary not only to choose properly the active medium, its geometry and doping ions, but also to elaborate the pump and cooling systems. Below, we consider successively all these aspects.

2. Choice of ions for the active medium

Crystals doped with trivalent Yb^{3+} and Nd^{3+} ions are most convenient active media for lasers emitting at ~1 μm. Both these media have their advantages and disadvantages.

The main advantage of ytterbium-doped crystals is the lower heat release in them compared to neodymium-doped crystals. Thus, the heat release in Nd : YAG crystals achieves 30 % – 35 % [5], while in Yb : YAG it is about 15 % [6]. The difference is explained by the fact that the quantum defect $\Delta E = h\nu_{\mathrm{p}} - h\nu_{\mathrm{L}}$ in Yb^{3+} ions is smaller than that in Nd^{3+} ions. However, the absorption cross section at the pump wavelength of ytterbium ions is also considerably lower than for neodymium ions (these cross sections for YAG crystals are $\sim 7 \times 10^{-21}$ cm^2 [7] and $\sim 6 \times 10^{-20}$ cm^2 [8], respectively). Therefore, to obtain efficient lasing, the concentration of ytterbium ions in the active medium should be high enough. At present the concentrations of Yb ions used in Yb : YAG crystals are about 10 % (see, for example, [9]). At such and higher concentrations of ytterbium in crystals grown by the Czochralski technique in iridium crucibles, a decrease in the luminescence lifetime of ytterbium due to quenching by impurities is observed [10], resulting in the enhanced heat release compared to the theoretical value. The method of growing crystals in rhenium crucibles [10], which allows the synthesis of heavily doped Yb : YAG crystals almost without quenching centres, has not received wide applications. In addition, as follows from experiments, even in the absence of concentration quenching, the best results are obtained at ytterbium concentrations lower than 10 %, which is probably related to the high threshold power at high Yb^{3+} concentrations.

Lasing in ytterbium-doped media occurs according to the quasi-four-level scheme with the low-lying final laser level (~610 cm^{-1} for Yb : YAG [11]). This leads to large values of the threshold lasing power and inverse population and also to a strong temperature dependence of lasing parameters. Lasing in Nd^{3+} ions occurs according to the classical four-level scheme, and therefore the temperature dependence of lasing parameters in this case is considerably weaker. In addition, a higher (compared to neodymium ions) inverse population leads to a large optical power of a Kerr lens [12], especially for high-average power lasers. Thermal and Kerr (electronic) lenses induced in the active element can be partially compensated by different methods: by a proper choice of the resonator design and geometry of the active element, adaptive optics, etc. However, a strong temperature sensitivity of the lasing parameters of Yb^{3+} ions requires cooling the active medium down to relatively low temperatures (see, for example, [13, 14]).

The advantages and disadvantages of Yb^{3+}- and Nd^{3+}-doped active media listed above show that neodymium-doped media are most promising for the development of high-power crystal lasers.

3. Possibilities of modern diode lasers for pumping

One of the key conditions for the development of high-power compact lasers is the realisation of the maximal possible pump power density. At present the output power emitted by a diode bar of size 10 mm × 1 μm amounts to 50 W. Therefore, the pump power required for operation of high-power lasers can be obtained either by assembling diode bars in diode arrays followed by focusing radiation to the active element (see, for example, [9, 15, 16]) or by using laser diode assemblies with a fibre pigtail (the power of a diode assembly at the output of a glass fibre pigtail of diameter 400 – 600 μm achieves 500 W). The choice of the method for obtaining the maximum pump power density absorbed in the active element depends on the element geometry and resonator design. The second method of pumping ranks below the direct-focusing method in the pump power loss due to the use of a double set of focusing optics, being, however, more flexible due to the separation of the pump system and active element. In this case, it is convenient to cool laser diodes and the active medium separately, and the mechanical design of the laser is simplified.

4. Choice of the active medium geometry

A laser beam is distorted and radiation is depolarised mainly due to the heating of the active medium. Therefore, the shape of the active element should be chosen to provide the best cooling conditions. In addition, it is desirable to provide the propagation of the laser beam through the active medium in such a way that aberrations caused by the inhomogeneous distribution of temperature in the active element would be minimal.

All other conditions being the same, the higher is the ratio of the area of a surface being cooled to the active element volume, the better is cooling of the active element. This requirement is best realised in two limiting cases of a thin plate with a large surface area or a long thin rod with a large length-to-diameter ratio (for example, in the case of fibre lasers).

The negative action of temperature effects in the active medium on the radiation quality can be minimised by using the waveguide propagation of radiation in the active element (in particular, the zigzag path of a laser beam in plates) or when the propagation direction of a laser beam coincides with the temperature gradient in the active element.

Waveguide lasers [16] and zigzag slab lasers [17] feature stable parameters in the output power range from 100 to 1000 W. A further increase in the output power requires fundamentally new technical solutions, which drastically complicate the laser design. In addition, a small cross-sectional area of active elements of fibre lasers restricts the possibility of Q-switching of such lasers.

On the other hand, the use of the active element in the form of a thin plate, in which the laser beam propagates perpendicular to its plane [14], allows one to increase easily the output power of the laser by increasing the beam cross section by preserving the pump power density.

Thus, the choice of the active element in the form of a thin neodymium-doped crystal plate with the transverse propagation of the laser beam in it is preferable. Below, we will perform estimates for such an active element.

5. Distributions of temperature and thermoelastic stresses in the active element

Practical restrictions appearing during the operation of any solid-state laser are caused first of all by temperature gradients produced in the active element.

Plate active elements can be cooled in two ways, either on both sides or on one side. If the heat release in the volume is homogeneous, the temperature profile in both cases is described by a parabola; however, the difference between the maximal and minimal temperatures is different and the maximal temperatures in the active element are also different.

The distribution of temperature in the stable regime can be found by solving the stationary heat conduction equation with boundary conditions (of the third kind in the general case).

Similarly to the method used in [18], we obtain the distributions of temperature and thermoelastic stresses in a thin disc pumped on one side ($x = 0$) and cooled on the other side ($x = h$, where h is the disc thickness), which are valid for any optical density of the active medium.

If the pump power incident on the active element is $P_{\rm p}$, then (by neglecting reflection from the active element surface and considering cooling only on one side of the plate) we obtain the expressions for the temperature increment $\Delta T(x) = T(x) - T(h)$ and thermoelastic stresses σ in the form

$$\Delta T(x) = \frac{\eta_{\rm t} P_{\rm p}}{k\lambda_{\rm t} S}\left(e^{-kh} - e^{-kx}\right) + \frac{\eta_{\rm t} P_{\rm p}}{\lambda_{\rm t} S}(h - x),$$

$$\sigma = \frac{\alpha E}{1-\nu}\frac{\eta_{\rm t} P_{\rm p}}{\lambda_{\rm t} S}\left[\frac{e^{-kx}}{k} + \frac{e^{-kh}}{hk^2} - \frac{1}{hk^2} + \left(\frac{12x}{h^3} - \frac{6}{h^2}\right)\right.$$
$$\left.\times\left(\frac{e^{-kh}h}{2k^2} + \frac{e^{-kh}}{k^3} + \frac{h}{2k^2} - \frac{1}{k^3}\right)\right],$$

where S is the area of the active element surface; $\eta_{\rm t}$ is the fraction of the absorbed pump power spent for heating the active element; k is the absorption coefficient of the active medium at the pump wavelength; $\lambda_{\rm t}$ is the thermal conductivity; α is the thermal expansion coefficient; E is Young's modulus; and ν is the Poisson ratio. We assume in calculations that the mechanical and thermal properties of the active medium are isotropic.

Figure 2 presents the results of calculations. For definiteness, the values of thermomechanical constants were taken equal to those for a YAG crystal.

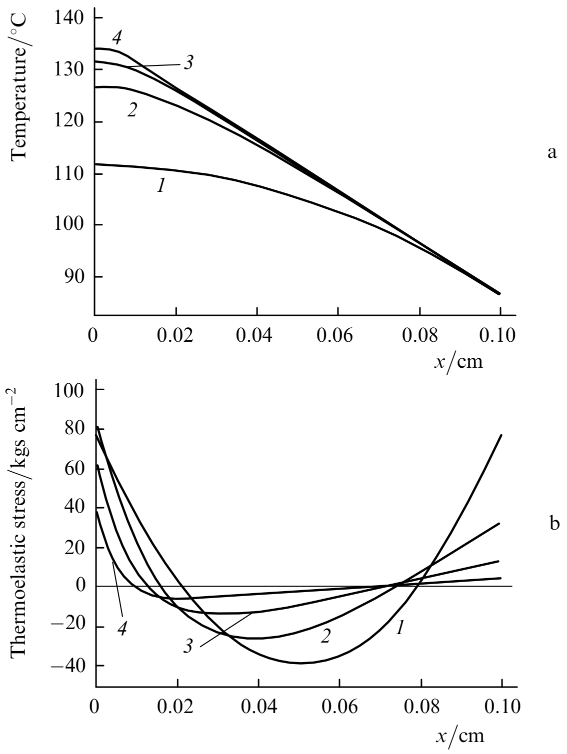

Figure 2. Distributions of temperature (a) and thermoelastic stresses (b) in active media of high-power disc crystal lasers for optical densities of the active medium $D = 0.1$ (*1*), 5 (*2*), 10 (*3*), and 20 (*4*), the disc area $S = 1000$ cm^2, thickness $h = 0.1$ cm, the thermal power dissipated in the disc 50000 W, and the cooling liquid temperature 20 °C.

We assumed in calculations that the total thermal power dissipated in a crystal is the same for all optical densities. One can see from Fig. 2 that the temperature distribution changes from the classical parabolic distribution at low optical densities ($D = 0.1$) to the 'quasi-linear' distribution at high optical densities ($D = 20$). The higher is D, the higher is the maximal temperature of a sample, but the larger is a linear interval in the dependence $T(x)$ and the lower are thermoelastic stresses, because it is known that stresses do not appear in the case of the linear dependence $T(x)$ [18]. One can also see that the maximal temperature of the active element is ~130 °C. We will show below that lasing parameters at such temperatures remain the same as at room temperature. Thus, the results obtained above show that:

(i) The heat release power being the same, the temperature drop between the planes of the active element in an optically dense medium is approximately twice that in a medium with uniformly distributed heat sources (i.e. in a medium with a low absorption coefficient);

(ii) as the optical density $D = kh$ is increased, the temperature distribution tends to a linear one;

(iii) maximal thermoelastic stresses are observed in the crystal plane irradiated by the pump beam. In this case, as the optical density D is increased, thermoelastic stresses decrease, which is explained by the fact that the temperature distribution in the sample approaches the linear distribution [18]. For the sample thickness $h = 1$ mm and $D > 6$, thermoelastic stresses become smaller than those for small D (the heat release power being the same).

6. Restrictions imposed on the active medium geometry by superluminescence and generation of parasitic modes

Consider now the main sources of excitation energy losses in neodymium-doped active media. First of all, they include losses due to the spontaneous decay of the $^4F_{3/2}$ level, superluminescence, and generation of parasitic modes. The necessary condition for a strong influence of the two latter factors is a combination of the high enough gain with a long optical path for superluminescence and parasitic modes in the active medium.

The excitation energy losses in neodymium-doped glass lasers and amplifies have been studied in detail (see, for example, references in [19]). The analytic expression

$$\frac{J_{\mathrm{ASE}}}{J_{\mathrm{s}}} = \frac{\Omega}{4}\frac{G_0}{\sqrt{\ln G_0}}$$

for the superluminescence power flow J_{ASE} as a function of the small signal gain was obtained in a number of papers, in particular, in [20]. Here, J_{s} is the saturation power flow; Ω is the solid angle within which luminescence propagates in the active element; $G_0 = \exp(g_0 l_{\mathrm{av}})$ is the total unsaturated (threshold) gain in the active medium; l_{av} is the path length of beams in the active element averaged over all the directions taking into account the zigzag propagation of a fraction of beams between the end-faces within the total internal reflection angle; and g_0 is the gain.

The appearance of lasing at parasitic modes in disc amplifiers has been also investigated in detail. For the beams propagating along a zigzag closed path in a disc and experiencing a number of total internal reflections from working surfaces and reflections from the side surface with the reflectance R_{ss}, the condition of the appearance of parasitic modes has the form [20]

$$R_{\mathrm{ss}} \exp\left(\frac{n_2}{n_1} g d_0\right) = 1,$$

where n_2 and n_1 are the refractive indices of the active material and environment on the working surfaces; g is the gain; and d_0 is the disc diameter.

In both cases, the probability of appearing parasitic effects strongly depends on the gain g if the active medium, which is determined in the simplest case from the threshold condition $2gh = L - \ln R_{\mathrm{out}}$, where L are total losses in the active element and R_{out} is the output mirror reflectance. A combined solution of equations specifying the conditions for appearing 'useful' lasing, generation of parasitic modes and superluminescence makes it possible to determine the critical relation between the disc thickness h and its diameter d_0. For cw lasing (the gain is low, $R_{\mathrm{out}} = 0.8 - 0.9$), the ratio $\beta = d_0/h$, which should not be exceeded, is $\sim$25, while this ratio for pulsed lasing should be even smaller.

7. Experimental results

Experimental results obtained by using optically dense active disc elements confirm the calculations and estimates made above. Figure 3 presents the scheme for measuring the temperature of active elements. Measurements were performed for a neodymium-doped lanthanum–scandium–borate crystal (Nd : LSB) and Ng : YAG and Nd : GdVO$_4$ crystals. The temperature $T_{\max}$ at the centre of the pumped region on the disc surface was determined by the number of interference rings that have 'run' over the crystal for the time from the beginning of pumping to the establishment of the stationary regime, while the number of rings determined the temperature drop ΔT over the sample. The pump power density incident on the sample was $\sim$30 kW cm^{-2} and the absorbed pump power density was $\sim$300 kW cm^{-3}. The values of $T_{\max}$ and ΔT are presented in Table 1.

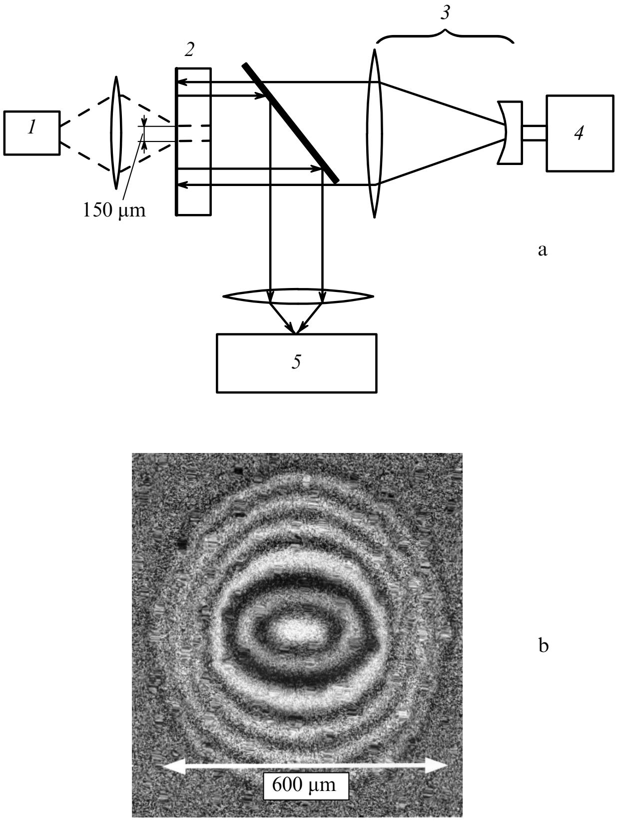

Figure 3. Scheme of the setup for studying the heating of disc active elements (a) and the interference ring pattern for the Nd : LSB crystal (b); (*1*) pump diode ($P = 1 - 2$ W); (*2*) active element of size $3 \times 3 \times 1$ mm; (*3*) telescope; (*4*) He–Ne laser; (*5*) CCD camera; dashed straight lines are the pump radiation, solid straight lines are radiation from a He–Ne laser.

Table 1. Heating of disc active elements made of neodymium-doped crystals.

Crystal	$\Delta T/{}^\circ$C	$T_{\max}/{}^\circ$C
Nd : YAG	15	90
Nd : GdVO$_4$	20	110
Nd : LSB	70	150

We found that the output power of these crystal lasers did not change at these temperatures, i.e. the heating of crystals up to rather high temperatures is not critical. Figure 4 presents the optical scheme of a diode-pumped Nd : GdVO$_4$ thin disc laser. The laser was pumped at 808 nm by a laser diode array with a pigtail (NA = 0.2). The reflectance of the output mirror at the laser wavelength of 1.064 μm was 94 %. The size of the crystal was $4 \times 4 \times 0.35$ mm, and the size of the pumped region of the active element was $\varnothing 0.2 \times 0.35$ mm. The volume density of the absorbed pump power was $\sim$400 kW cm^{-3}. The crystal was cooled by circulating water.

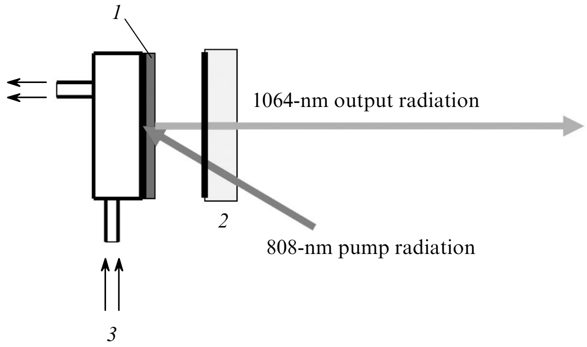

Figure 4. Scheme of a diode-pumped Nd : GdVO$_4$ thin disc laser; (*1*) active element of size $4 \times 4 \times 0.35$ mm; (*2*) output mirror ($R_{\rm out} = 94$ %); (*3*) circulating water cooling.

Figure 5 shows the dependence of the output power density on the absorbed power density. We did not optimise the lasing efficiency in these experiments and it was 26 %. Such an optimisation for the Nd : GdVO$_4$ laser provides the lasing efficiency up to 70% [21]. The ratio of the diameter d of the pumped region to the crystal thickness h was 0.6. If we assume that $d/h = 20$, which corresponds to the required conditions providing acceptable losses related to parasitic modes and superluminescence, then the pump spot diameter for this pump power density can achieve 6 mm. This will provide the output power up to $1-2$ kW. Then, for the readily obtained lasing efficiency of 50 % and the output power 1.5 kW, the required pump power will be 3 kW. Analysis shows that, to obtain multikillowatt powers, the diameter of the active element should be considerably greater than the value required by the restriction $d_0/h \leqslant 25$, which is caused by losses related to parasitic modes and superluminescence. This discrepancy can be eliminated by using the multichannel, i.e. spatially separated, scheme for pumping the active medium by dividing a thin disc of a large diameter into sections, for example, by the method of ion etching (Fig. 6).

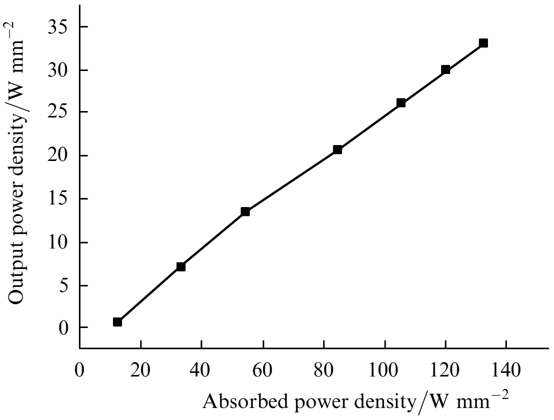

Figure 5. Dependence of the output power density on the absorbed power for the Nd : GdVO$_4$ thin disc laser.

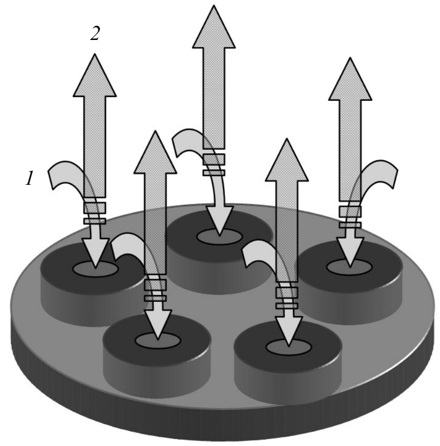

Figure 6. Sectional disc active element based on the multichannel-pumped dense active medium: (*1*) pump radiation; (*2*) laser radiation; the coherent combination of laser beams is performed in the common resonator of the laser.

At present the computer simulation of a multikilowatt laser is being performed, which includes the simulation of the development of oscillation in the high-power laser with stable or unstable resonators and the calculation of a setup consisting of a master oscillator and a multichannel multipass amplifier.

The aim of calculations is to determine the laser beam quality (comparison of its divergence with the diffraction-limited value) and the factor of filling the medium by radiation. The calculations are performed by using the Fresnel software package developed at the General Physics Institute, RAS [22], which allows one to take into account the resonator geometry, the inhomogeneous pump power distribution, gain saturation, amplitude and phase distortions in the active medium, and incoherent initiating spontaneous radiation.

8. Conclusions

Thus, we have shown in this paper that thin discs with a high optical density are promising active elements for the development of diode-pumped multikilowatt lasers. We have found that the use of optically dense media makes it possible to perform single-pass pumping of thin discs and minimises thermal loads. The multichannel scheme for pumping active media has been proposed. Our experiments have demonstrated the possibility of the development of a multikilowatt laser by using neodymium-doped thin vanadate crystal discs.

Acknowledgements. The authors thank A.N. Alpat'ev and I.V. Epatko for useful discussions and M.B. Stukan and D.K. Sychev for their help in the preparation of the paper.

References

1. Heller A., in *Science & Technology Review* (Livermore, 2006, April) pp 10 – 17.
2. Goodno G.D., Komine H., McNaught S.J., et al. *Opt. Lett.*, **31**, 1247 (2006).
3. Alpat'ev A.N., Danilov A.A., Nikol'skii M.Yu., Prokhorov A.M., Zvetkov V.B., Shcherbakov I.A. *Trudy IOFAN*, **26**, 107 (1990).
4. Jenssen T., Meyn J.-P., Huber G., Ostroumov V.G., Zagumennyi A.I., Shcherbakov I.A. *Tech. Dig. CLEO-93* (Baltimore, 1993) p. 590.
5. Brown D.C. *IEEE J. Quantum Electron.*, **34**, 560 (1998).
6. Vetrovec J. *Materials for High-Average Power Solid-State Lasers. Preprint of a paper 4968-9 presented at LASE 2003 Conf.* (San Jose, Cal, 2003).
7. Chenais S., Druon F., Balembois F., et al. *Opt. Mater.*, **22**, 99 (2003).
8. Xionghui Zeng, Guangjun Zhao, Xiaodong Xu, et al. *J. Cryst. Growth*, **274**, 106 (2005).
9. Yanagisawa T., Yamamoto S., Hirano Y., in *OSA Trends in Optics and Photonics on Advanced Solid-State Lasers* (Washington, D.C., OSA, 2004) Vol. 94, p. 242.
10. Petermann K., Fagundes-Peters D., Johannsen J., et al. *J. Cryst. Growth*, **275**, 135 (2005).
11. Yoshikawa A., Boulon G., Laversenne L., Canibano H., Lebbou K., Collombet A., Guyot Y., Fukuda T. *J. Appl. Phys.*, **94**, 5479 (2003).
12. Antipov O.L., Bredikhin D.V., Eremeykin O.N., Savikin A.P., Ivakin E.V., Sukhadolau A.V. *Opt. Lett.*, **31**, 763 (2006).
13. Karszewski M., Brauch U., Erhard S., et al., in *OSA Trends in Optics and Photonics on Advanced Solid-State Lasers* (Washington, D.C., OSA, 1998) Vol. 19, p. 296.
14. Erhard S., Giesen A., et al., in *OSA Trends in Optics and Photonics on Advanced Solid-State Lasers* (Washington, D.C., OSA, 1999) Vol. 26, p. 38.
15. Takada A. et al., in *OSA Trends in Optics and Photonics on Advanced Solid-State Lasers* (Washington, D.C., OSA, 1999) Vol. 26, pp 21 – 23.
16. Lee J.R. et al., in *OSA Trends in Optics and Photonics on Advanced Solid-State Lasers* (Washington, D.C., OSA, 2001) Vol. 50, p. 36.
17. Tulloch W.M., Rutherford T.S., Gustfson E.K., Byer R.L., in *OSA Trends in Optics and Photonics on Advanced Solid-State Lasers* (Washington, D.C., OSA, 1999) Vol. 26, p. 9.
18. Podstrigach Ya.S., Kolyano Yu.M. *Obobshchennaya termomekhanika* (Generalised Thermomechanics) (Kiev: Naukova Dumka, 1976).
19. Mak A.A., Soms L.N., Fromzel' V.A., Yashin V.E. *Lazery na neodimovom stekle* (Neodymium Glass Lasers) (Moscow: Nauka, 1990).
20. Linford G.J., Pressini E.R., Sooy W.R., Spaeth M.L. *Appl. Opt.*, **13**, 379 (1974).
21. Zavartsev Yu.D., Zagumennyi A.I., Kalachev Yu.L., et al. *Kvantovaya Elektron.*, **37**, 315 (2007) [*Quantum Electron.*, **37**, 315 (2007)].
22. Epatko I.V., Serov R.V. *J. Phys. IV*, **133** (1), 679 (2006).